Relation between thermal history, structural relaxation and glass forming ability of an amorphous alloy in the chalcogenide ternary system As–Se–Te

R.A. Ligero [a],*, M. Casas-Ruiz [a], A. Orozco [a], M.P. Trujillo [b], R. Jiménez-Garay [b]

[a] *Facultad de Ciencias Náuticas, Universidad de Cádiz, Puerto Real, Spain*
[b] *Facultad de Ciencias, Universidad de Cádiz, Puerto Real, Spain*

Abstract

A sample of the alloy $As_{47}Se_6Te_{47}$ has been subject to an aging process at room temperature for two years and to different annealings at intermediate temperatures between the glass transition and crystallization temperatures. By means of DSC calorimetric techniques the further crystallization reactions were studied, computing the parameters E, n, y, K_0, which describe their kinetic behaviour. From the analysis of the calorimetric curves and the evolution of the mentioned parameters, some hypotheses about the structural relaxation in the material have been achieved, in line with the type of crystal growth deduced. Two parameters for computing the glass forming ability (GFA) showed their effectiveness, bearing out the hypotheses about structural relaxation.

Keywords: Alloy; Chalcogenide; DSC; Glass forming ability; Kinetics; Relaxation; Ternary system

1. Introduction

The chalcogenide glasses show some properties which make them a very useful material for the development of devices for technological application [1,2].

The crystallization plays a very important role in the determination of the stability of these materials and their possible practical applications [3].

* Corresponding author.

Differential scanning calorimetry is a widely used technique in the study of the crystallization kinetics of amorphous materials. To get a complete understanding of this kind of phase transitions a wide set of factors must be borne in mind, some of which are the structure of the material, the age of the sample and its thermal history.

This work gives a study about the modifications in the crystallization process of an alloy of the glassy system As–Se–Te, subject first to aging, and later to annealings at different temperatures, and the mentioned changes are related with the short range order postulated for the material.

2. Experimental

The alloy was made from high purity (5N) elements which, in suitable proportions, were ground to a grain size of less than 64 µm, sealed at vacuum (0.0001 Torr) in a quartz ampoule and held in a furnace at 800°C for 24 h, rotating at 1/3 rpm in order to guarantee homogeneity, and subsequently quenched in ice-water at 0°C. The amorphous nature of the samples was confirmed using a Siemens D-500 X-ray powder diffractometer.

The calorimetric measurements were carried out by a Perkin-Elmer D-7 differential scanning calorimeter, on 4–5 mg samples ground to grain size of less than 64 µm, and held in crimped aluminium pans. Empty aluminium capsules were used as reference.

The calorimetric technique was by continuous heating at constant heating rates of 2, 4, 8, 16 and 32 K min^{-1}, and samples analysed were previously subject to different thermal treatment: as-quenched sample (M0), aged at room temperature during two years (M1), and annealed at 401 K (M2), at 404 K (M3), at 407 K (M4), at 410 K (M5), and at 413 K (M6).

Table 1 shows the experimental magnitudes obtained for the different samples, where ΔH is the heat of the crystallization process, T_g is the glass transition temperature, T_{on} is the onset temperature, and T_p is the temperature corresponding

Table 1
Experimental values obtained for different samples

Sample	$\Delta H/(\text{J mol}^{-1})$	T_g/K	First stage		Second stage	
			T_{on}/K	T_p/K	T_{on}/K	T_p/K
M0	47.65	405	433	438	–	–
M1	50.16	393	435	441	494	503
M2	52.25	396	431	438	490	501
M3	50.16	399	429	437	488	502
M4	48.07	401	419	432	489	499
M5	28.01	401	413	432	489	500
M6	13.1	401	411	431	485	494

to the maximum of the exothermic crystallization peak. These data were obtained as the average of the values from the calorimetric scans at different experimental heating rates.

3. Kinetics of the processes

The analysis of the crystallization reaction kinetics of the samples was realized accepting the usual Johnson–Mehl–Avrami model, from which we get [4]

$$x = 1 - \exp[-(Kt)^n] \tag{1}$$

where x is the volumetric crystallized fraction, t is the effective crystallization time, n is the order of the reaction or Avrami index, and K the reaction constant rate, which is allowed to obey an Arrhenius expression for the absolute temperature T

$$K(T) = K_0 \exp(-E/RT) \tag{2}$$

where E is the activation energy of the crystallization process, and K_0 is the pre-exponential factor or frequency factor.

It is generally assumed that the knowledge of the parameters E, n and K_0 gives a satisfactory approximation for the mechanism which governs the kinetics of the crystallization reactions, although recently this has been questioned owing to the uncertainty in the simultaneous computing of the parameters [5,6].

Under certain restrictions, the theoretical outcomes obtained for isothermal conditions may not be valid when applied to continuous heating calorimetric experiences [7].

There exist several methods for computing the above mentioned parameters [8–10] and in the present we will use that described by Gao and co-workers [11,12], for which, in the case when $E \gg RT$, the following relations are fulfilled

$$\beta \frac{E}{K_p R T_p^2} = 1 \tag{3}$$

$$\left. \frac{dx}{dt} \right|_p = 0.37 n K_p \tag{4}$$

$$\frac{d[\ln(dx/dt)_p]}{d(1/T)} = -\frac{E}{R} \tag{5}$$

where β is the heating rate, and where the subscript p refers to the values of the variables at the crystallization peak.

If the values of $(dx/dt)_p$ can be identified in a series of exotherms taken at different heating rates, the plots of $\ln(dx/dt)_p$ versus $1/T_p$ should be a straight line with a slope $(-E/R)$.

The set of Eqs. (3) and (4) allows us to obtain the kinetic parameters n and K_0 taking the average of the values calculated for every heating rate. Table 2 shows the results obtained for the samples subject of this work.

Table 2
Parameters calculated using Eqs. (3) and (4)

Sample	First stage			Second stage		
	$E/(kJ\ mol^{-1})$	n	K_0	$E/(kJ\ mol^{-1})$	n	K_0
M0	163.3	2.7	5.3×10^{17}	--	–	
M1	138.4	3.4	3.2×10^{14}	147.6	3.4	2.3×10^{13}
M2	120.8	3.2	3.5×10^{12}	134.6	3.5	3.4×10^{12}
M3	137.1	2.5	4.8×10^{14}	118.3	3.5	2.5×10^{10}
M4	146.7	1.7	8.5×10^{15}	150.1	3.1	5.8×10^{13}
M5	144.6	1.5	5×10^{15}	150.1	3.1	6×10^{13}
M6	150.5	1.3	2.9×10^{16}	153.0	3.2	1.3×10^{14}

4. Glass forming ability

We can find in the literature several criteria to evaluate the glass forming ability (GFA) of the amorphous materials and, even although some of them have an absolute character, they describe the relative ability of a set of compounds to adopt the amorphous structure.

In practice, the criteria to establish the thermal stability of vitreous materials are based on DSC calorimetric measurements. Usually, unstable glasses show a crystallization peak near to the glass transition temperature, though for stable glasses the peak is closer to the melting temperature. Thus, glass forming ability can be evaluated by means of the difference between the crystallization temperature (peak temperature or onset temperature) and the glass transition temperature T_g. It has been observed that, in general, this difference varies with the composition, taking a maximum for a certain composition range which appears to give the best glasses.

To make quantitative comparisons among glasses with different T_g, it is usual to normalize the aforementioned thermal difference by dividing by T_g to get an adimensional parameter for measuring the GFA. Here, we will compare the GFA of samples of one alloy with different thermal histories, in order to see its effect on the mentioned property.

Some authors determine the GFA through thermodynamic criteria related to the reaction heat [13]; others use criteria related to the crystallization kinetic parameters [14,15]; we have proposed a way to evaluate the GFA through the rate constant $K_p = K(T_p)$ [16]; Hruby [17] introduced a function of the characteristic temperatures of the reaction $K_{gl} = (T_p - T_g)/(T_1 - T_p)$, where T_1 is the liquidus temperature; and Saad and Poulain [18] have widely discussed like best criterium the function $S = (T_p - T_{on})(T_{on} - T_g)/T_g$, where T_{on} is the onset temperature of the peaks. Table 3 shows the calculated values for the two last parameters of the GFA from the studied samples.

5. Analysis of the results

Fig. 1 shows the crystallization peaks of the analysed samples with their different thermal history. We can notice at first that the as-quenched sample showed just one crystallization stage, whereas the aged at room temperature and the annealed samples at different temperatures crystallize in two thermally well separated stages. This can be interpreted if we remember that the original amorphous sample does not have a high thermal stability, and that time changes their structural units.

Fig. 1 shows also that annealing has less influence in the crystallization reaction corresponding to the second stage than in the first one. In the latter the DSC curves
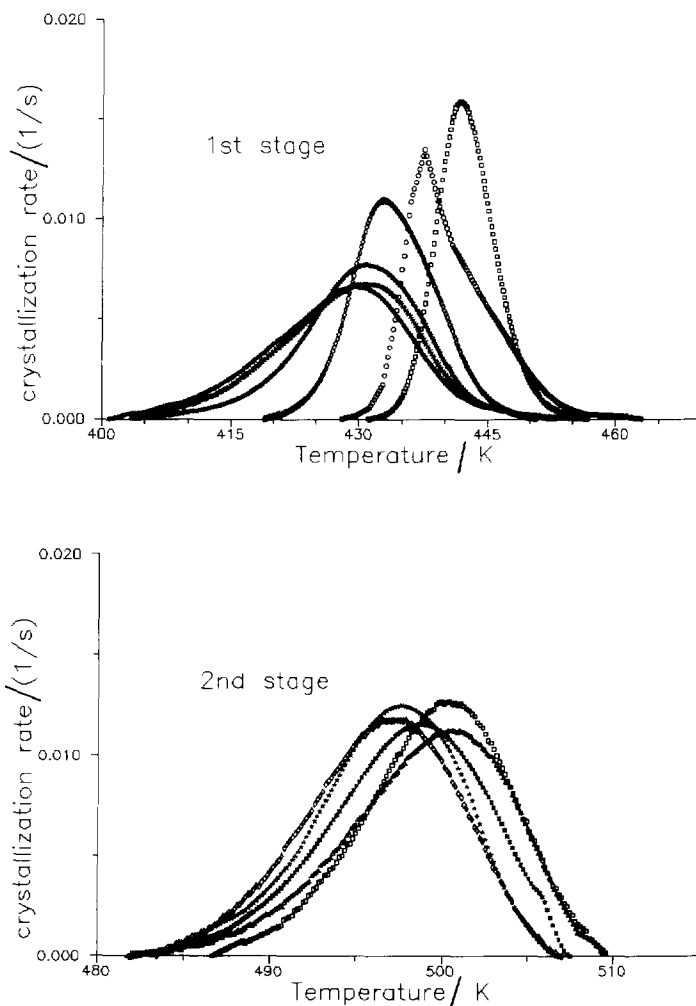
Fig. 1. DSC curves of the studied sample for their different thermal history corresponding to a heating rate of 8 K min $^{-1}$: ○, as-quenched; □, aged; △, at 401 K; ◇, at 404 K; ★, at 407 K; ×, at 410 K; and * at 413 K.

suffer a shift to lower temperatures as annealing temperature increases, whereas the second stage does not.

Likewise, the shape of the crystallization peaks of the first stage changes substantially with the thermal treatment of the sample, and otherwise, the shape of the peaks corresponding to the second ones are very similar.

Keeping in mind all the above, we can say that the qualitative variation in the enthalpy of the crystallization processes is restricted just to the first peak of the reactions, neglecting the influence on it of the second stage of the reactions. This is revealed in Fig. 2, where we see the rapid decrease of the enthalpy of the process as the annealing temperature of the sample rises, as shown by the behaviour (size, shape and position) of the DSC curves of the first peak.

Fig. 3 shows the plots of crystallized fraction versus time for the first stage of all the experimental reactions to which the samples have been subjected. We can observe the following in them.

Table 3
Calculated values for parameters of GFA

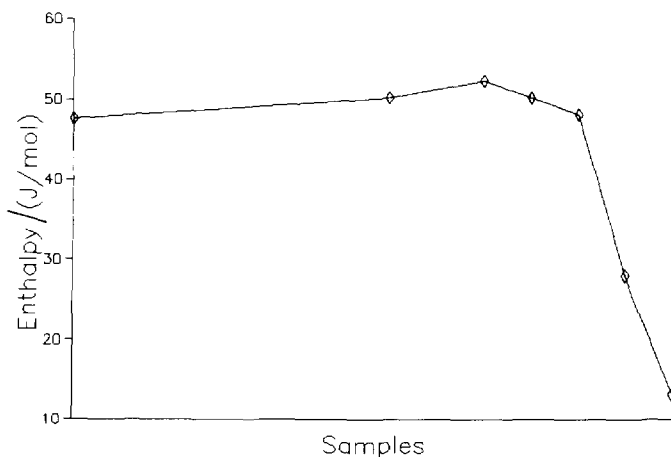| Sample	First stage		Second stage	
	K_{gl}	S	K_{gl}	S
M0	0.194	0.345	–	–
M1	0.322	0.641	1.26	2.31
M2	0.269	0.620	1.13	2.61
M3	0.242	0.601	1.06	3.12
M4	0.182	0.584	0.95	2.19
M5	0.183	0.569	0.98	2.41
M6	0.181	0.499	0.87	1.89

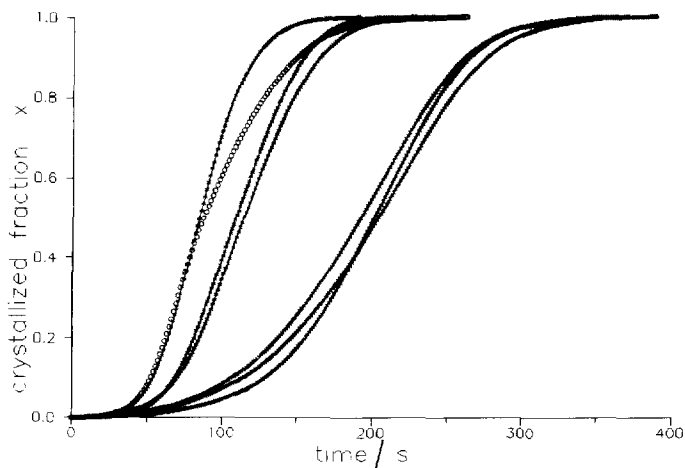Fig. 2. Enthalpy of the crystallization reactions of samples with different thermal histories.

Fig. 3. Plots of the crystallized fraction versus time (first stage) for a heating rate of 8 K min^{-1}: ○, as-quenched; □, aged; △, at 401 K; ◇, at 404 K; ★, at 407 K; ×, at 410 K; and *, at 413 K.

(a) The induction time raises with increase of annealing temperature. From the calculated values for the reaction order, and according to the usual interpretation for this parameter [19], it can be concluded that annealing favours crystallization with linear growth ($n \approx 1$), which obviously slows down the volumetric transformation of the material.

(b) The behaviour of the aged sample is the same that the as-quenched sample in the first part of the crystallization reaction ($x \leq 0.47$). After this point, the crystallization of the aged sample occurs more quickly than for the as-quenched sample.
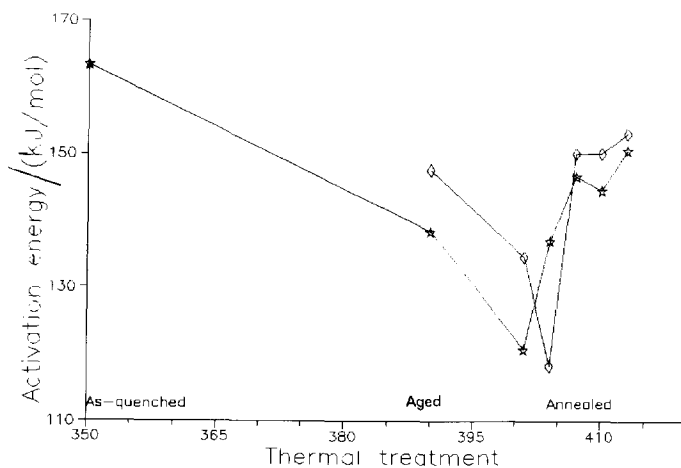

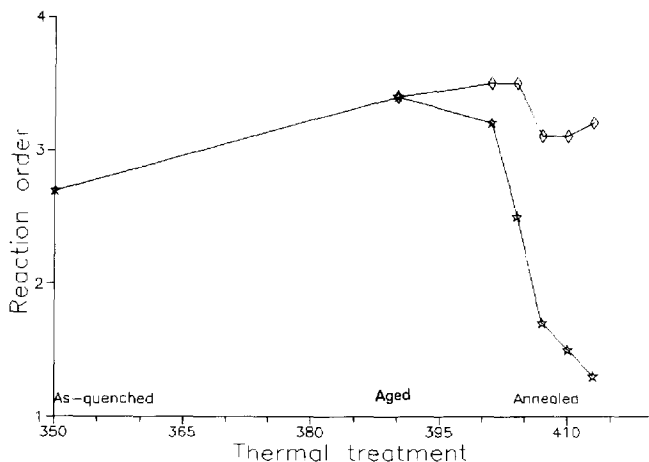Fig. 4. Activation energy versus thermal history of the sample ☆, first stage; ◇, second stage.

Fig. 5. Reaction order of the crystallization reaction versus thermal history of the sample: ☆, first stage; ◇, second stage.

(c) An important influence of the previous annealing in the behaviour of the samples disappears after the second heating (at 403 K). From then on, all the crystallization reactions are similar, as confirmed by the calculated values for the kinetic parameters.

Fig. 4 shows the constancy of the activation energy for the last three thermal treatments (≈ 150 kJ mol^{-1}).

Fig. 5 plots the reaction order versus thermal treatment of the sample, and in it we can notice that, for the same thermal history, the Avrami index tends to 1 in the
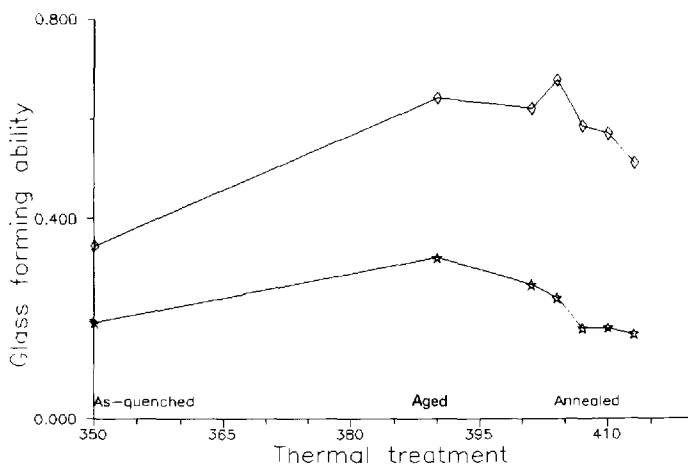

Fig. 6. Glass forming ability of the samples with different thermal histories for the first stage of the crystallization reaction: ☆, K_{gl}; ◇, S.

first crystallization peak, and stays about 3 for the second peak, in agreement with the above comments about the stability of the last.

In the model of structure proposed for alloys of this system with similar compositions [20], one may observe basic units made up of tetrahedrons centred on tetra-coordinated As atoms, and triangular pyramids in one of whose vertices there is a tri-coordinated As atom. These basic units are joined together directly, or by analogous pyramidal units based on Te atoms. Lateral chains, made up of bi-coordinated Se and Te atoms, are also observed to connect the mentioned basic units. Bearing in mind all of the above, and the straightforwardness of Te to form linear chains, the observed tendency of the index n, after the successive thermal treatments of the sample, seems to confirm that aging at room temperature and annealing favour the formation of linear chains based on tellurium. These chains would be the principal subject of the first crystallization stage, whereas the more closed and stable structural units based in pyramids and tetrahedrons will form the crystallization nuclei with tri-dimensional growth which characterize the second stage.

The evaluation criteria of the GFA of amorphous samples are simple and they are successful when the material shows just one crystallization stage. However, they are more difficult to interpret when the crystallization is carried out in several stages. At this case, it is usual to consider just the first crystallization peak or, more rarely, an average among the different peaks. However, glasses showing close stability parameters behave quite differently according to whether they are thin, ribbon or bulk samples, so that the vitreous stability of a material which crystallizes in a complex form can only be compared among samples of similar shape and size.

Fig. 6 shows the plots of parameters K_{gl} and S for the first stage of our samples. From its study, we deduce that the aged sample has reached more thermal stability
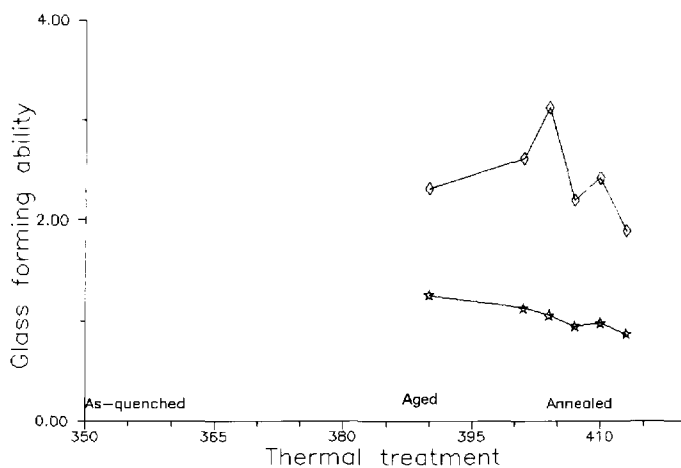

Fig. 7. Glass forming ability of the samples with different thermal histories for the second stage of the crystallization reaction: ☆, K_{gl}; ◇, S.

compared with the as-quenched sample, and the successive heatings cause a loss of the vitreous character of the sample, according with the shift towards the glass transition temperature and the change in the shape of the corresponding DSC curves.

Fig. 7 shows the same parameters evaluated for the second stage of the reaction. The remarkable rise in their value in relation to the earlier ones confirms the high stability of this stage. The practical constancy of K_{gl} and S for the different heatings is also in agreement with the similarity noted in the DSC curves, and both parameters are satisfactory in order to evaluate the GFA.

6. Conclusions

The aging and annealing cause a structural relaxation in the sample which separate the later crystallization into two stages characterized by one-dimensional growth and three-dimensional growth, respectively.

The evolution of the kinetic parameters describing the crystallization reactions with the thermal history of the material has become a good procedure to verify structural hypotheses derived from other kinds of analysis.

Although it is not always easy to evaluate the GFA of a glassy alloy displaying complex crystallization reactions, the parameters K_{gl} and S are effective for comparing the thermal stability of the two crystallization stages which occur in the studied sample.

References

[1] M.D. Rechtin, A.R. Hilton and D.J. Hayes, J. Elect. Mater., 4(2) (1975).
[2] S.R. Ovshinsky, J. Non-Cryst. Solids, 73 (1985) 395.
[3] S.R. Ovshinsky, in D. Adler, B.B. Schwartz and M.C. Steele (Eds.), Physical Properties of Amorphous Materials, Plenum Press, New York, 1985.
[4] M. Avrami, J. Chem. Phys., 7 (1939) 1103; 8 (1940) 212; 9 (1941) 177.
[5] S.V. Vyazovkin, Thermochim. Acta, 211 (1992) 181.
[6] S.V. Vyazovkin and A.I. Lesnikovich, Thermochim. Acta, 182 (1991) 133.
[7] T.J.W. De Bruijn, W.A. de Jong and P.J. van der Berg, Thermochim. Acta, 45 (1981) 315.
[8] J.A. Augis and J.E. Bennet, J. Therm. Anal., 13 (1978) 283.
[9] M.E. Kissinger, J. Res. Natl. Bur. Stand., 57 (1956) 217.
[10] R.A. Ligero, J. Vázquez, P. Villares and R. Jiménez-Garay, J. Mater. Sci., 26 (1991) 211.
[11] Y.Q. Gao and W. Wang, J. Non-Cryst. Solids, 81 (1986) 129.
[12] Y.Q. Gao, W. Wang, F.-Q. Zhen and X. Liu, J. Non-Cryst. Solids, 81 (1986) 135.
[13] B.T. Kolomiets, Phys. Status Solidi A, 7 (1964) 713.
[14] D.R. Uhlmann, J. Non-Cryst. Solids, 7 (1972) 337.
[15] S. Suriñachs, M.D. Baró and M.T. Clavaguera-Mora, J. Non-Cryst. Solids, 111 (1989) 113.
[16] R.A. Ligero, J. Vázquez, P. Villares and R. Jiménez-Garay, Mater. Lett., 8 (1989) 6.
[17] A. Hruby, Czech. J. Phys. B, 22 (1972) 1187.
[18] M. Saad and M. Poulain, Mat. Sci. Forum, 19–20 (1987) 11.
[19] J.W. Christian, in The Theory of Transformation in Metal and Alloys, Pergamon, New York, 2nd edn., 1975.
[20] R.A. Ligero, M. Casas-Ruiz, J. Vázquez and P. Villares, J. Mater. Sci., 27 (1992) 1001.